Isolation and Structure of Halistatin 1 from the Eastern Indian Ocean Marine Sponge *Phakellia carteri*[1]

George R. Pettit,*,† Rui Tan, Feng Gao, Michael D. Williams, Dennis L. Doubek, Michael R. Boyd,‡ Jean M. Schmidt, Jean-Charles Chapuis, Ernest Hamel,§ Ruoli Bai,§ John N. A. Hooper,⊥ and Larry P. Tackett

Cancer Research Institute and Department of Chemistry, Arizona State University, Tempe, Arizona 85287-1604, Laboratory of Drug Discovery Research and Development, DTP, DCT, National Cancer Institute, Frederick Cancer Research and Development Center, Frederick, Maryland 21702-1201, Laboratory of Molecular Pharmacology, DTP, DCT, National Cancer Institute, Bethesda, Maryland 20892 and Queensland Museum, So. Brisbane, QLD 4101, Australia

Received August 31, 1992

A highly potent new polyether macrolide antimitotic agent designated halistatin 1 (**5**) was isolated (8.8×10^{-7}% yield) from *Phakellia carteri*. The marine sponge was located in coastal areas of the Republic of the Comoros, and it was also found to contain halichondrin B (**3**) and homohalichondrin B (**4**). Structure elucidation of halistatin 1 (**5**) was achieved primarily by employing extensive high-field (400- and 500-MHz) 2D NMR techniques. Halistatin 1, like halichondrin B and homohalichondrin B, caused the accumulation of cells arrested in mitosis, inhibited tubulin polymerization, and inhibited the binding of radiolabeled vinblastine and GTP to tubulin.

Indo-Pacific Porifera are proving to be a productive source of new cytotoxic macrolides bearing complex pyran systems. Illustrative (with KB and L-1210 cell lines showing ED_{50} responses in the range 1.0–to 10^{-2} μg/mL) are the swinholides[2] (cf. 1) and the closely related misakinolide A[3] (and bistheonellides[4]), isolated from *Theonella* species of Okinawan marine sponges. Another interesting series of Porifera pyran derivatives constitute the calyculins.[5,6] Four of the latter compounds (e.g., **2**) even proved lethal to the German cockroach at 10 μg/male specimen and to mosquito larvae at 10 ppm.[7] The fused pyran–spiroketal molecular types characteristic of halichondrin B (**3**) and homohalichondrin B (**4**) have exhibited remarkably potent antineoplastic activities.[8-10] We have reported[9] isolation of these two powerfully antineoplastic polyether macrolides (**3**, **4**) from a new Western Pacific (Palau) marine sponge in the genus *Axinella*.

Marine sponges in the Axinellida order (class Demospongiae) constitute eight families of generally yellow-orange species with a distinct axial component that may grow to 50 cm or more. The *Phakellia* genus of the Axinellidae family is quite typical. In the fall of 1987 we collected 250 kg (wet wt) of the orange *Phakellia carteri* in the Republic of Comoros. Methanol extracts of this Western Indian Ocean sponge provided confirmable activity against the P388 lymphocytic leukemia (PS system). The P388 cell line bioassay was used to guide the isolation and purification of pure active constituents. The results summarized here concern discovery of a new polyether macrolide designated halistatin 1 (**5**) that showed highly potent cytotoxic activity in vitro against P388 cells (ED_{50} 4×10^{-4} μg/mL) and against human cancer cells comprising the U.S. National Cancer Institute's (NCI) 60-cell line antitumor screening panel[11-13] (average overall panel GI_{50} 7×10^{-10} M).

The sponge was preserved in methanol upon collection. In 1989 the liquid phase was removed and diluted with dichloromethane followed by water. Bioassay showed PS ED_{50} 0.74 μg/mL for the dichloromethane phase. The methanol–water layer proved to be inactive. The dichloromethane fraction was separated by partition between hexane and methanol–water (9:1),[9] followed by partition between dichloromethane and methanol–water (3:2). The cytostatic activity was again located in the dichloromethane fraction (ED_{50} 0.22 μg/mL, Scheme I).

Separation (Schemes I–III) of the bioactive dichloromethane fraction by bioassay-directed (PS) Sephadex LH-20 column chromatography was conducted beginning with gel permeation (methanol) followed by partition (3:2 dichloromethane–methanol and hexane–toluene–metha-

† Arizona State University.
‡ National Cancer Institute, Frederick, MD.
§ National Cancer Institute, Bethesda, MD.
⊥ Queensland Museum, Australia.

(1) Part 250 in the sequence Antineoplastic Agents. Contribution 249 appears as: Pettit, G. R.; Cichacz, Z.; Barkozcy, J.; Dorsaz, A. C.; Herald, D. L.; Williams, M. D.; Doubek, D. L.; Schmidt, J. M.; Tackett, L. P.; Brune, D. C.; Cerny, R. L.; Hooper, J. N. A. *J. Nat. Prod.* **1993**, *56*, 260.

(2) Kobayashi, M.; Tanaka, J.; Katori, T.; Kitagawa, I. *Chem. Pharm. Bull.* **1990**, *38*, 2960–2966. Tsukamoto, S.; Ishibashi, M.; Sasaki, T.; Kobayashi, J. *J. Chem. Soc. Perkin Trans. 1* **1991**, 3185–3188.

(3) Tanaka, J.; Higa, T.; Kobayashi, M.; Kitagawa, I. *Chem. Pharm. Bull.* **1990**, *38*, 2967–2970.

(4) Kobayashi, J.; Tsukamoto, S.; Tanabe, A.; Sasaki, T.; Ishibashi, M. *J. Chem. Soc., Perkin Trans. 1* **1991**, 2379–2383.

(5) Kato, Y.; Fusetani, N.; Matsunaga, S.; Hashimoto, K.; Fujita, S.; Furuya, T. *J. Am. Chem. Soc.* **1986**, *108*, 2780–2781.

(6) Kato, Y.; Fusetani, N.; Matsunaga, S.; Hashimoto, K. *J. Org. Chem.* **1988**, *53*, 3930–3932.

(7) Okada, A.; Watanabe, K.; Umeda, K.; Miyakado, M. *Agric. Biol. Chem.* **1991**, *55*, 2765–2771.

(8) Uemura, D.; Takahashi, J.; Yamamoto, T.; Katayama, C.; Tanaka, J.; Okumura, Y.; Hirata, Y. *J. Am. Chem. Soc.* **1985**, *107*, 4796–4798. Hirata, Y.; Uemura, D. *Pure Appl. Chem.* **1988**, *58*, 701–710.

(9) Pettit, G. R.; Herald, C. L.; Boyd, M. R.; Leet, J. E.; Dufresne, C.; Doubek, D. L.; Schmidt, J. M.; Cerny, R. L.; Hooper, J. N. A.; Rützler, K. C. *J. Med. Chem.* **1991**, *34*, 3339–3340.

(10) Bai, R.; Paull, K. D.; Herald, C. L.; Malspeis, L.; Pettit, G. R.; Hamel, E. *J. Biol. Chem.* **1991**, *266*, 15882–15889.

(11) Boyd, M. R. Status of the NCI preclinical antitumor drug discovery screen: Implications for selection of new agents for clinical trial. In *CANCER: Principles and Practice of Oncology Updates*, DeVita, V. T., Jr., Hellman, S., Rosenberg, S. A., Eds.; J. B. Lippincott: Philadelphia, 1989; Vol. 3, No. 10, pp 1–12.

(12) Monks, A.; Scudiero, D.; Skehan, P.; Shoemaker, R.; Paull, K.; Vistica, D.; Hose, C.; Langley, J.; Cronise, P.; Vaigro-Wolff, A.; Gray-Goodrich, M.; Campbell, H.; Boyd, M. *J. Natl. Cancer Inst.* **1991**, *83*, 757–766.

(13) Boyd, M. R.; Paull, K. D.; Rubinstein, L. R. Data display and analysis strategies for the NCI disease-oriented in vitro antitumor drug screen. In *Antitumor Drug Discovery and Development*; Valeriote, F. A., Corbett, T., Baker, L., Eds.; Kluwer Academic: Amsterdam, 1991; pp 11–34.

0022-3263/93/1958-2538$04.00/0 © 1993 American Chemical Society

Chart I

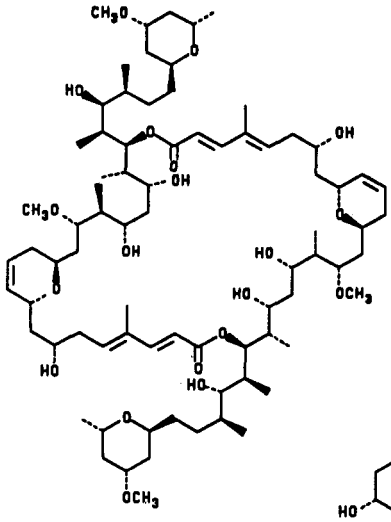

1
SWINHOLIDE-A

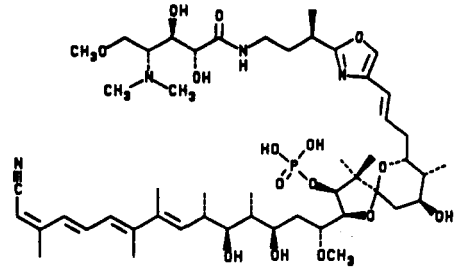

2
CALYCULIN A

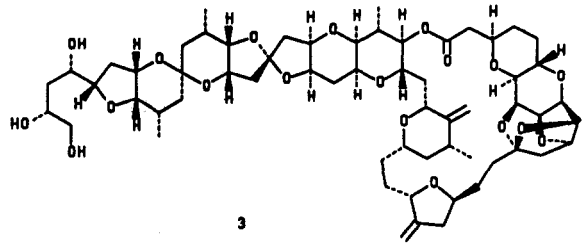

3
HALICHONDRIN B

Chart II

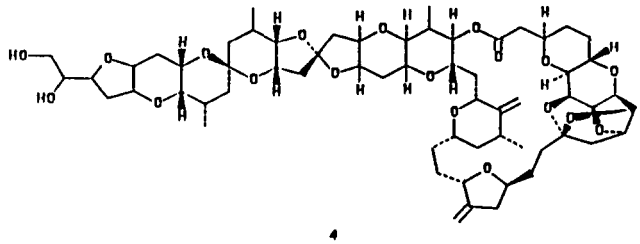

4
HOMOHALICHONDRIN B

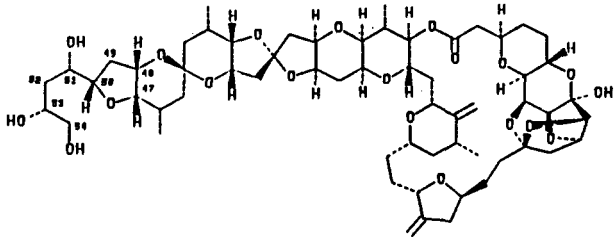

5
HALISTATIN 1

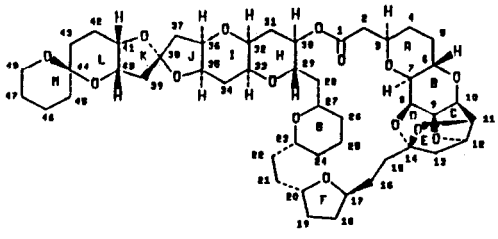

6
HALIPYRAN

nol (3:1:1)) sequences. Three PS active fractions from the latter chromatograms were identified (Scheme I). Fraction III (2.5 g, ED_{50} 0.03 μg/mL) was separated (Scheme II) three times on a Sephadex LH-20 column with hexane–2-propanol–methanol (8:1:1), hexane–ethyl acetate–methanol (9:2:1), and heptane–chloroform–ethanol (7:4:1) as eluent to yield fraction C4 (10 mg) with PS ED_{50} 0.0029 μg/mL. Further separation of fraction C4 was realized by reversed-phase silica gel HPLC with methanol–acetonitrile–water (5:5:6) and detection by refractive index. The major component exhibited a sharp peak and represented halistatin 1 (**5**, 2 mg, 8×10^{-7}% yield).

Bioactive fraction I was partition chromatographed on a Sephadex LH-20 column using hexane–2-propanol–methanol (8:1:1). The principal PS active fraction was subjected to high speed countercurrent distribution using a hexane–ethyl acetate–methanol–water (1:1:1:1) system followed by reversed-phase silica gel HPLC, to give (7.6 mg, 3.4×10^{-6}%) homohalichondrin B (**4**). Halichondrin B (**3**) was isolated (8 mg, 3.5×10^{-6}% yield) from fraction II as summarized in Scheme III.

The structure elucidation of halistatin 1 (**5**) was mainly accomplished by 2D NMR (Table I) and mass spectral analyses. The molecular formula $C_{60}H_{86}O_{20}$ was established by FAB high-resolution mass spectrometry which revealed 1126 as the molecular weight with the molecular ion peak at 1149.5621 $[M + Na]^+$: calcd for $C_{60}H_{86}O_{20}Na$, 1149.5632. The IR spectrum showed carbonyl absorption at 1736 cm^{-1}, unconjugated double bonds at 1653 cm^{-1} (sharp, weak), and ether absorptions at 1186, 1080, and 1018 cm^{-1} (strong). Comprehensive analysis of ^1H-NMR, ^1H–^1H COSY, APT, HMQC, and ^{13}C-NMR spectra located four methyl groups (δ 0.96/18.15; 1.01/18.35; 1.05/15.84; 1.09/18.42), 19 methylenes (one attached directly to oxygen at δ 3.52, 3.45/67.20), 28 methines (24 bonded to oxygens), two vinylidene units (δ 5.07, 5.01/105.70; 4.87, 4.81/104.80; 153.33; 153.22), four quaternary carbons, and one carbonyl group. These interpretations suggested a polyether macrolide skeleton assembled reminiscent of the halichondrin series.

Scheme I

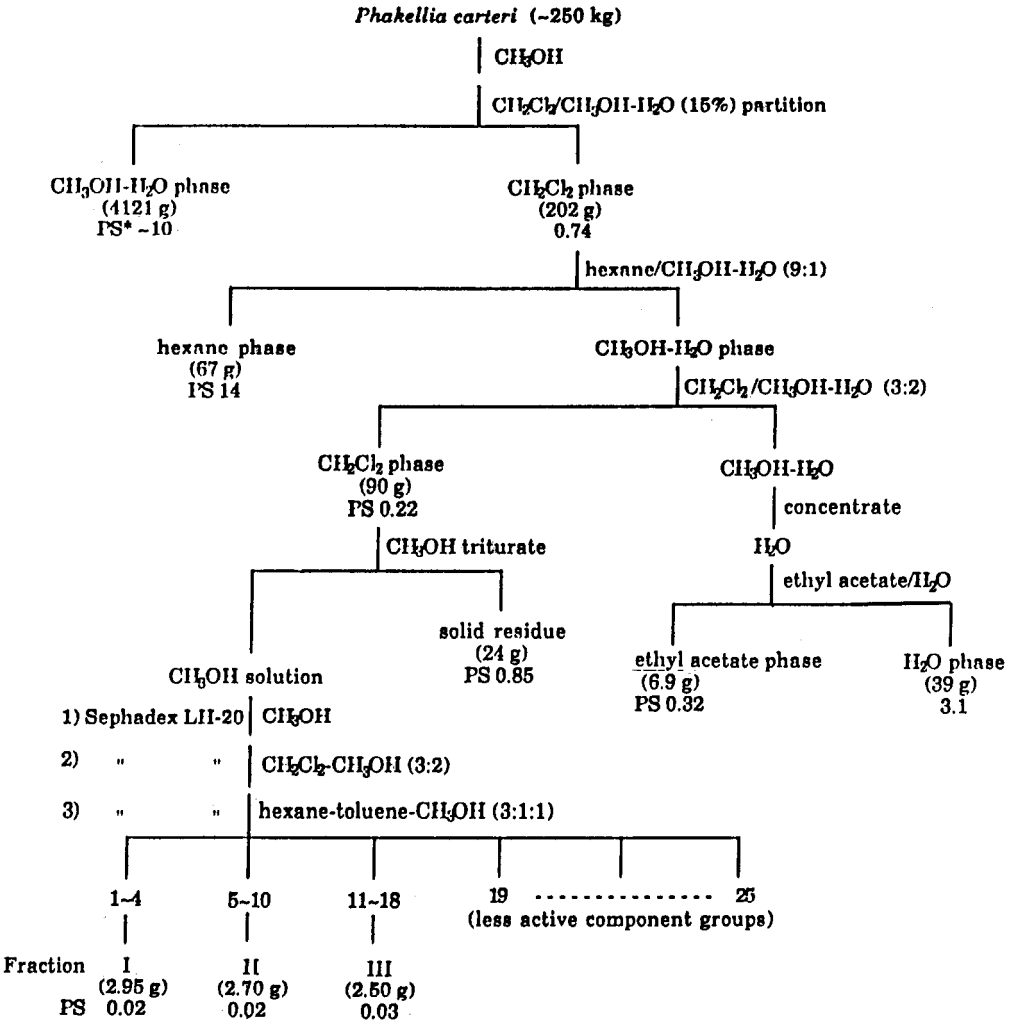

* PS=P388 ED_{50} in μg/ml

Scheme II

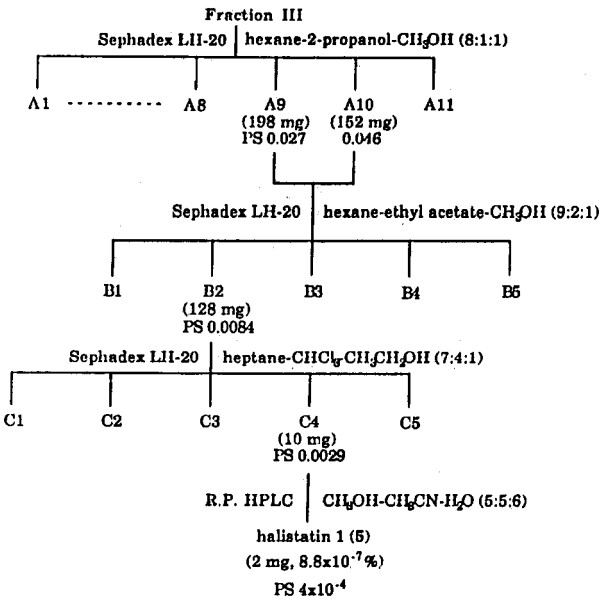

The ^{1}H-NMR spectrum of halistatin 1 superficially resembled that of halichondrin B (4). In the ^{1}H–^{1}H COSY spectrum of halistatin 1, the signal at δ 4.74 (triplet, J = 4.6 Hz) evidenced couplings with the signal at δ 4.25 (broadened doublet, J = 4.4 Hz) and an upfield signal at δ 1.96 (doublet of doublets, J = 13.3, 4.6 Hz) (Table I). The latter signal showed strong coupling with another upfield signal at δ 2.12 (broadened doublet, J = 13 Hz). From the chemical shift, coupling pattern, and coupling constants, the signal at δ 4.74 was attributed to H-12 and the signals at δ 1.96 and 2.12 to H-13. In the COSY spectrum, the coupling pattern and chemical shift of the signals at δ 4.25 and 3.75 (doublet of doublets, J = 4.3, 1.5 Hz) suggested that the C-10 proton was missing. Such an analysis was supported by the ^{13}C NMR spectrum where a new quaternary carbon signal attributed to a hemiketal was observed at δ 103.75. In agreement with a hemiketal group at C-10, signals for the C-9 and C-11 carbons were shifted downfield (δ 6.5 ppm and 3.8 ppm, respectively). In the ^{1}H-NMR spectrum, the signals for H-9 and H-11 showed 0.4 ppm and 0.35 ppm upfield shifts, respectively. The ^{1}H- and ^{13}C-NMR signals for the other atoms were essentially the same as those of halichondrin B (4). Here, it is worth noting that H-11 showed small couplings with H-9 (δ 3.75) and one of the two H-13 (δ 2.12) protons, which were explained by W-couplings. Indeed, a Dreiding molecular model indicated that W-couplings should be present between H-11 and H-9, as well as between H-11 and one of the H-13 protons. An HMBC spectrum

Scheme III

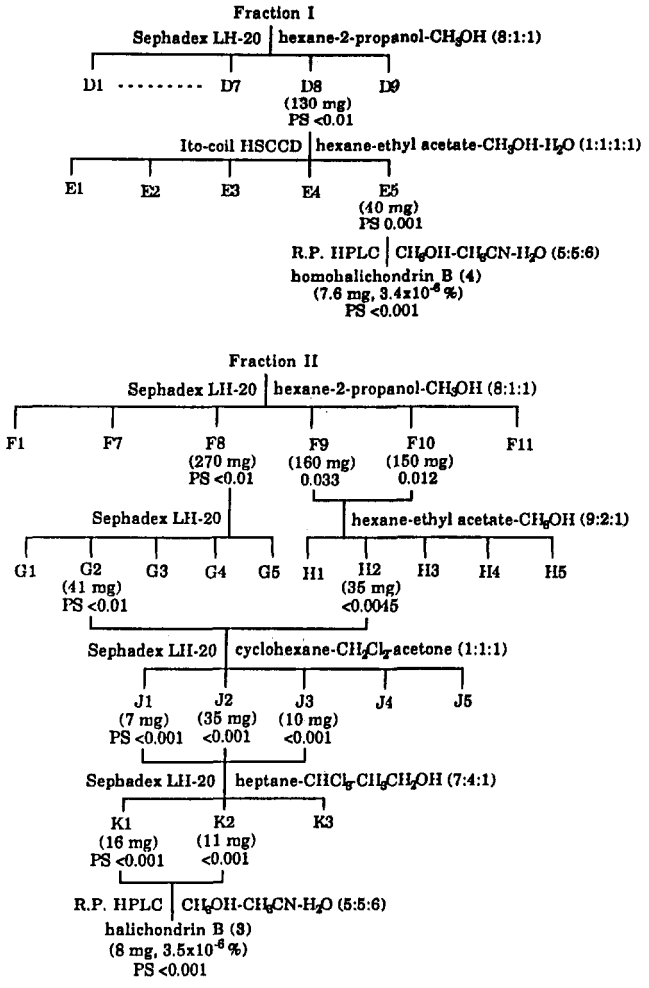

recorded at 500 MHz also strongly supported structure **5** for halistatin 1.

The ^{13}C signal at δ 103.75 (C-10) showed a correlation with ^{1}H signals at δ 3.75 (H-9), 4.25 (H-11), 4.23 (H-8), and 4.74 (H-12). The ^{13}C signals at δ 87.64 (C-11) showed cross peaks at δ 3.75 (H-9), 2.12 (H-13), 4.74 (H-12). Furthermore, the ^{13}C signal at δ 110.83 (C-14) showed cross peaks at δ 4.25 (H-11), 4.74 (H-12), 1.96, 2.12 (H-13), 4.23 (H-8). Other cross peaks agreed with the proposed structure **5** (see Table I for details). No attempt was made to assign every methylene signal due to severe overlapping of the ^{1}H signals. However, ^{13}C signals for 18 methylene groups in the δ 50–28 ppm region were observed. The asymmetric centers of halistatin 1 were assumed to be the same as those of halichondrin B. The optical rotation was similar, $[\alpha]_D = -58.4°$ (lit.[8] $[\alpha]_D$ −58.9° for halichondrin B); Since Dreiding molecular models indicated that a β-hydroxyl group was not sterically possible in such a condensed ring system, the hydroxyl group at the C-10 was assigned the α-orientation to complete the structural elucidation of halistatin 1 (**5**). In turn, this overall assignment is based on an X-ray crystal structure determination of a norhalichondrin derivative.[8] Halichondrin C[8b] appears to be a structural isomer of halistatin 1. For example, in the ^{13}C NMR spectrum of halistatin 1, the signals at δ 79.77 (C-9) 103.75 (C-10), and 82.32 (C-12), differ from those reported[8b] for halichondrin C: δ 73.3 (C-9), 73.0 (C-10), and 114.2 (C-12). Also, in the ^{1}H NMR spectrum of halistatin 1, a triplet signal at δ 4.74 (J = 4.6 Hz could only be assigned to the 12-H. This signal showed umambiguous couplings with the signal at δ 4.25 (broadened doublet, J = 4.4 Hz) and a high-field signal at δ 1.96 (doublet of doublets, J = 13.3, 4.6 Hz) which were assigned to 11-H and 13-H, respectively. Due to the increasing importance[9] and frequency of occurrence of the halichondrins the name halipyran is henceforth recommended for the unsubstituted ring system (A) and the halistatin core for our present member (**5**) as well as a forthcoming new series of strongly antineoplastic active derivatives.

With L1210 murine leukemia cells halistatin 1 and halichondrin B had similar cytotoxicity (IC_{50} values of 0.5 and 0.2 nM, respectively), and both agents caused a significant rise in the mitotic index at cytotoxic concentrations, reaching values as high as 21% for halistatin 1. In the glutamate-induced polymerization of purified tubulin, performed as described previously,[10] halistatin 1 was slightly more active than halichondrin B (IC_{50} values of 4.6 ± 0.4 and 4.9 ± 0.5 μM, respectively). Halichondrin B has been shown to be a noncompetitive inhibitor of the binding of radiolabeled vinblastine to tubulin and to inhibit nucleotide exchange on tubulin.[10] A comparison of halistatin 1 with halichondrin B in these two assays indicated that halistatin 1 had activity comparable to halichondrin B as an inhibitor of vinblastine binding, but that halistatin 1 was superior as an inhibitor of nucleotide exchange. Comparing the two drugs at 5 and 10 μM, halistatin 1 inhibited the binding of radiolabeled vinblastine by 57 and 73% at the two concentrations, as compared with 51% and 73% with halichondrin B. For radiolabeled GTP binding to tubulin, the same drug concentrations inhibited the reaction by 12% and 37% with halistatin 1 and by 14% and 18% with halichondrin B. Comparable values obtained previously[10] with halichondrin B did not differ significantly from those obtained in the current studies.

When tested in the U.S. National Cancer Institute's in vitro primary screen,[11-13] halistatin 1 yielded a pattern of differential cellular growth inhibition which was highly characteristic and of comparable potency to the halichondrins (**3**, **4**).[9,10] Computerized pattern-recognition analyses revealed that the mean graph profiles of halistatin 1 and halichondrins 3 and 4 were all strongly correlated with each other and also with the profiles of a general class of tubulin-interactive antimitotics. The latter class includes known clinically active anticancer agents such as the vinca alkaloids and taxol. On the basis of these biological properties, and the differences in the chemistry reported herein, comparative in vivo evaluations of halistatin 1 with the available known in vivo active halichondrins are warranted. This is further reinforced by the NCI Decision Network Committee's recent selection of halichondrin B as representative of a new chemotype for anticancer drug development.[14] While the recently reported[15] total synthesis of halichondrin B appears to offer a promising future source of the parent compound, and possibly also important derivatives thereof, the continued search for new natural sources of the halichondrins/halistatins[16] and related bioactive structures remains an urgent priority for current drug development initiatives.

(14) NCI Decision Network Committee minutes, March 23, 1992, NCI, Bethesda, MD.
(15) Aicher, T. D.; Buszek, K. R.; Fang, F. G.; Forsyth, C. J.; Jung, S. H.; Kishi, Y.; Matelich, M. C.; Scola, P. M.; Spero, D. M.; Yoon, S. K. *J. Am. Chem. Soc.* **1992**, *114*, 3162–3164.
(16) Pettit, G. R.; Gao, F.; Doubek, D. L.; Boyd, M. R.; Hamel, E.; Schmidt, J. M.; Tackett, L. P.; Rützler, K. *Gazz. Chim. Ital.*, in press.

Table I. Halistatin 1 (5) NMR Assignments Recorded in Deuteriomethanol with Tetramethylsilane as Internal Standard[a]

carbon no.	^{13}C (100 MHz)	HMQC (500 MHz)		HMBC (500 MHz)
CO-1	172.86p			H-30, H-2, H-3
CH_2-2	41.20p	2.55 (dd, 18/9.6)	2.45 (dd, 18/3)	H-3
CH-3	74.99n	3.89 (m)		H-2
CH_2-4	31.62p	1.72	1.35	H-2
CH_2-5	31.49p	2.08	1.50	
CH-6	71.21n	4.44		H-7, H-8
CH-7	78.84n	3.06 (dd, 10/2)		H-6, H-8
CH-8	75.10n	4.23 (dd, 4.5/2)		H-6, H-7, H-9
CH-9	79.77n	3.75 (dd, 4.3/1.5)		H-12, H-11, H-7
C-10	103.75p			H-12, H-11, H-8, H-9
CH-11	87.64n	4.25 (brd, 4.4)		H-12, H-9, H-13
CH-12	82.32n	4.74 (t, 4.6)		H-11, H-9, H-13
CH_2-13	49.10p	2.12 (d, 13)	1.96 (dd, 13.3/4.6)	
C-14	110.83p			H-11, H-8, H-12, H-13, H-15
CH_2-16	29.40p	2.15	1.42	H-18
CH-17	77.27n	4.04 (m)		H-16, H-18
CH_2-18	39.74p	2.80 (m)	2.31	H-19a
C-19	153.22p			H-18, H-17, H-20, H-19a
$=CH_2$-19a	105.70p	5.07 (d, 1.5)	5.01 (d, 1.5)	
CH-20	76.09n	4.44 (dd, 10/1.5)		H-19a
CH-23	75.41n	3.70		H-27, H-24
CH_2-24	44.99p	1.72	1.00 (m)	H-25a
CH-25	37.22n	2.29		H-23, H-24, H-25a, H-26a
CH_3-25a	18.42n	1.09 (d, 6.4)		
C-26	153.33p			H-27, H-25a, H-24, H-26a
$=CH_2$-26a	104.80p	4.87 (d, 1.5)	4.81 (d, 1.5)	H-27
CH-27	75.15n	3.60 (brd, 11.1)		H-26a, H-29
CH_2-28	37.85p	2.26	1.81	H-27
CH-29	73.84n	4.22 (m)		H-27, H-33
CH-30	77.45n	4.61 (dd, 7.5/4.6)		H-29, H-32, H-31a
CH-31	37.50n	2.05		H-29, H-30, H-31a, H-32
CH_3-31a	15.84n	1.05 (d, 7.0)		H-30, H-31, H-32
CH-32	78.08n	3.21 (dd, 6.6/4.7)		H-30, H-31a, H-33
CH-33	65.74n	3.87		H-29, H-32, H-35, H-31
CH_2-34	30.90p	2.07	1.83	H-32
CH-35	76.36n	4.10		H-33, H-37
CH-36	78.02n	4.10		H-32
CH_2-37	45.58p	2.39 (dd, 13/5.9)	2.02 (dd, 13/4)	
C-38	114.90p			H-40, H-37
CH_2-39	44.99p	2.34	2.34	
CH-40	73.05n	4.04 (brs)		H-41
CH-41	80.81n	3.70 (dd, 8/3)		H-40, H-42a
CH-42	27.18n	2.27 (m)		H-42a
CH_3-42a	18.15n	0.96 (d, 7.0)		H-41
CH_2-43	37.98p	1.50	1.30	H-42a, H-41
C-44	98.47p			H-45
CH_2-45	37.98p	1.52	1.44	H-46a
CH-46	27.13n	2.36		H-46a
CH_3-46a	18.35n	1.01 (d, 7.0)		H-47
CH-47	81.32n	3.56 (brs)		H-48, H-46a
CH-48	73.38n	4.09		H-47
CH_2-49	36.31p	2.26 (m)	1.81 (m)	
CH-50	81.29n	3.99 (ddd, 8.5/4.7/3)		H-49
CH-51	73.19n	3.78 (dt, 8/4)		H-53
CH_2-52	37.57p	1.75	1.59	H-50, H-53, H-54
CH-53	71.70n	3.86		H-51, H-54
CH_2-54	67.20p	3.52 (dd, 11/4.4)	3.45 (dd, 11.3/6.2)	H-53

[a] In entry marked by the signal for carbon-13 was overlapped with solvent signals and the chemical shift was estimated. Some of the coupling patterns and/or coupling constants were not measured due to overlapping. For the coupling constants refer to (Hz), and the n and p notations correspond to APT results in which n indicated one or three protons attached and p indicated none or two protons attached.

Experimental Section

General Methods. All solvents were redistilled. Sephadex LH-20 (25–100 μm) was employed for gel permeation and partition chromatography. High-speed countercurrent distribution (HSCCD) employed a horizontal coil planet centrifuge (P.C. Inc.) with the planet gear drive at 450 rpm. The HSCCD column (no. 10) consisted of 2.6-mm i.d. PTFE tubing with a volume of 350 mL. Solvent was delivered at a flow rate of 380 mL/h. A Prepex 5-20μ C 8 (reversed-phase) column (250 × 10 mm) was used for HPLC with a refractive index detector. Silica gel GHLF Uniplates were used for TLC. The TLC plates were viewed under UV light or by spraying with ceric sulfate–sulfuric acid solution followed by heating near 200 °C for 2 min.

FAB high-resolution mass spectra (Kratos MS 50) were obtained by the Midwest Center for Mass Spectrometry at the University of Nebraska. NMR experiments were conducted with Varian Unity 500-MHz, Bruker AM-400-MHz, and Varian Gemini 300-MHz instruments, with deuteriomethanol as solvent and tetramethylsilane as internal standard.

***Phakellia carteri* Collection and Initial Extraction.** The orange sponge *Phakellia carteri* was collected (400 L amounting to ~250 kg wet wt) at various locations along the reef on the south and southeast side of Grand Comoros Island, Republic of Comoros during October and November, 1987. The sponge was found in moderately high to high current areas from −12 to −37 m, primarily near the base of reefs or slopes. In appearance the firm textured sponge was lamellate with a small holdfast.

The membrane areas and interior were a lighter orange. Specimens were up to 12 cm in height, ridged and sintered with randomly placed oscula of 2 mm. The sponge (voucher specimens deposited in the ASU-CRI and Queensland Museum) was preserved and shipped in methanol (280 L). In July 1989, dichloromethane (200 L) was added followed by enough water (42 L) to cause phase separation. The dichloromethane layer was evaporated to dryness. The residue (202 g) showed bioactivity against the P388 lymphocytic leukemia cell line (PS) at ED_{50} 0.74 μg/mL. The methanol–water phase was essentially inactive with PS ED_{50} >10 μg/mL (Scheme I).

Solvent Partition Sequence. In August 1990, the dichloromethane fraction (202 g) was dissolved in methanol–water (9:1) and extracted with hexane. The methanol–water phase was then diluted to 3:2 and extracted with dichloromethane. Methanol was evaporated in vacuo from the methanol–water layer, and the aqueous solution was extracted with ethyl acetate. The resulting hexane (67 g), dichloromethane (90 g), ethyl acetate (6.9 g), and water (39 g) fractions were concentrated and bioassayed (PS). Again, the dichloromethane fraction was found to contain the active components (PS ED_{50} 0.22 μg/mL).

Isolation of Halistatin 1. The 90-g PS active dichloromethane fraction (Scheme I) was triturated with methanol (1100 mL), the solid phase was collected, and the solution was concentrated to 800 mL. The solution was chromatographed on a column of Sephadex LH-20 and eluted with methanol. The principal active fractions were combined and again chromatographed on a column of Sephadex LH-20 eluted with dichloromethane–methanol (3:2) followed by rechromatography of the PS active fractions and elution with hexane–toluene–methanol (3:1:1) to give active fractions I–III.

Guided by PS bioassay results, fraction III (2.5 g, PS ED_{50} 0.03 μg/mL) was further separated (refer to Scheme II) by a series of Sephadex LH-20 column chromatographic steps using as successive elution solvents hexane–2-propanol–methanol (8:1:1), hexane–ethyl acetate–methanol (9:2:1), and heptane–chloroform–methanol (7:4:1). The highly active fraction C4 (10 mg, PS ED_{50} 0.0029 μg/mL) was next separated using HPLC techniques with a C8 reversed-phase column and a flow rate of 0.8 mL/min with a methanol–acetonitrile–water (5:5:6) system to yield 2 mg of halistatin 1 (5): amorphous solid, $[\alpha]^{25}_D$ −58.4 (*c*, 0.57, CH_3OH); IR ν_{max} (film) 3406, 2928, 1736, 1653, 1437, 1335, 1277, 1186, 1080, 1018, 889, and 754 cm^{-1}; HRFABMS *m/z* 1149.5621 $[M + Na]^+$, calcd for $C_{60}H_{86}O_{20}Na$ 1149.5632; FABMS *m/z* 1165.5 $[M + K]^+$, 1149.5 $[M + Na]^+$, 1127.5 $[M + H]^+$, 883, 507, 307, 154. The 400-MHz proton and 100-MHz carbon magnetic resonance data have been listed in Table I.

Isolation of Homohalichondrin B (4). Nine PS-active fractions were obtained from the Sephadex LH-20 column chromatography of bioactive fraction I (2.95 g, PS ED_{50} 0.02 μg/mL) with hexane–2-propanol–methanol (8:1:1) as the mobile phase. Fraction D8 (see Scheme III), with high activity (0.13 g, PS ED_{50} <0.01 μg/mL), was separated using a high-speed countercurrent distribution technique (Ito coil) with the top layer from hexane–ethyl acetate–methanol–water (1:1:1:1, aqueous layer stationary) as mobile phase. By this means, the bioactive constituent was concentrated in the stationary phase (fraction E5). An aliquot of E5 (40 mg) was purified by reversed-phase HPLC (Prepex C8 column) with methanol–acetonitrile–water (5:5:6) elution to give homohalichondrin B (7.6 mg): $[\alpha]^{23}_D$ −80.7 (*c*, 0.15, CH_3OH). The ^1H- and ^{13}C-NMR spectral data corresponded to those of authentic homohalichondrin B.[8]

Isolation of Halichondrin B (3). Bioactive fraction II (2.7 g, PS ED_{50} 0.02 μg/mL Scheme I) was subjected to Sephadex LH-20 partition column chromatography and elution with hexane–2-propanol–methanol (8:1:1, Scheme III). Two active fractions (F8, F9) were further chromatographed separately on a Sephadex LH-20 column with hexane–ethyl acetate–methanol (9:2:1). Fractions from G2 and H2 were combined on the basis of TLC and bioassay results and were successively column chromatographed on Sephadex LH-20 using cyclohexane–dichloromethane–acetone (1:1:1) and then heptane–chloroform–ethanol (7:4:1). The resulting fractions K1 and K2 were separated by HPLC as described above (cf. 4) to provide 8 mg of halichondrin B (3): $[\alpha]^{23}_D$ −60.0 (*c*, 0.20, CH_3OH). Comparison of the ^1H-NMR (400-MHz) spectra in various deuterated solvents with those of authentic halichondrin B[9] showed no differences.

Biological Testing: Data Analysis and Summary. Pure compounds were tested in the NCI's human tumor, disease-oriented in vitro screen,[11-13] and data calculations were performed as described elsewhere.[13] The negative $\log_{10}$ GI_{50} values representing the averages obtained from quadruplicate screenings of halistatin 1 are listed as follows with the individual cell line identifiers: CCRF-CEM (9.43), HL-60TB (9.48), K-562 (9.44), MOLT-4 (9.21), RPMI-8226 (9.32), SR (9.50); A549/ATCC (8.54), EKVX (8.33), HOP-18 (8.00), HOP-62 (9.08), HOP-92 (8.96), NCI-H226 (9.09), NCI-H23 (9.24), NCI-H322M (8.46), NCI-H460 (9.40), NCI-H522 (9.68), LXFL 529 (9.32); DMS 114 (9.48), DMS 273 (9.54); COLO 205 (9.37), DLD-1 (8.92), HCC-2998 (8.89), HCT-116 (9.30), HCT-15 (8.38), HT29 (9.38), KM12 (9.24), KM20L2 (9.28), SW-620 (9.40); SF-268 (8.66), SF-295 (9.96), SF-539 (9.44), SNB-19 (8.64), SNB-75 (9.54), SNB-78 (9.32), U251 (9.29), XF 498 (9.32); LOX IMVI (10.09), MALME-3M (9.68), M14 (9.21), M19-MEL (9.54), SK-MEL-2 (9.54), SK-MEL-28 (9.11), SK-MEL-5 (9.80), UACC-257 (9.07), UACC-62 (9.57); IGROVI (9.08), OVCAR-3 (9.60), OVCAR-4 (8.15), OVCAR-5 (9.31), OVCAR-8 (8.72), SK-OV-3 (9.33); 786-0 (9.16), A498 (8.85), ACHN (8.49), CAKI-1 (8.80), RXF-393 (9.52), SN12C (8.66), TK-10 (8.22), UO-31 (8.21). At 40 μg/kg halistatin 1 led to a 330% increase in life span against the P388 in vivo leukemia.

Acknowledgment. The essential financial support for this investigation was provided by Outstanding Investigator Grant CA 44344-01A1-04 and PHS Grant CA-16049-09-12 awarded by the Division of Cancer Treatment, National Cancer Institute, DHHS, the Fannie E. Rippel Foundation, the Arizona Disease Control Research Commission, the Robert B. Dalton Endowment Fund, Eleanor W. Libby, the Waddell Foundation (Donald Ware), Virginia Piper, Polly J. Trautman, the Eagles Art Ehrmann Cancer Fund, and the Ladies Auxiliary, VFW, Department of Arizona. For other very helpful assistance we thank the Republic of Comoros (Damir Ben Ali, Mohammed Chaher, Karl Danga, W. R. Carlson), Drs. Ronald L. Cerny, Cherry L. Herald, Fiona Hogan-Pierson, Ronald A. Nieman, Bruce E. Tucker, Denise Nielsen-Tackett, Mr. William Schultz, Mr. Lee Williams, Mrs. Kim M. Weiss, the U.S. National Science Foundation (Grants CHE-8409644 and BBS-88-04992) and the NSF Regional Instrumentation Facility in Nebraska (Grant CHE-8620177).

Supplementary Material Available: ^1H and ^{13}C NMR spectra for halistatin 1 (2 pages). This material is contained in libraries on microfiche, immediately follows this article in the microfilm version of the journal, and can be ordered from the ACS; see any current masthead page for ordering information.